EXPERIMENTAL VALIDATION OF CROSS-SECTIONAL ANALYSIS FOR COMPOSITE ROTOR BLADES

I. J. Park[1], M. K. Dhadwal[2], S. N. Jung[3]*, D. H. Kim[4]
[1,2,3] Department of Aerospace Information Engineering, Konkuk University, Seoul, Republic of Korea, [4] Rotor Department, Korea Aerospace Research Institute, Daejeon, Republic of Korea
* Corresponding author (snjung@konkuk.ac.kr)

Keywords: *cross-section analysis, finite element method, shear center, rotor blades*

1 Introduction

Helicopter rotor blades are generally composed of solid and/or thin-walled cross-section which consists of complex geometries and various topologies such as erosion shield, skin, spar and balancing weight. The blades are usually modeled as one-dimensional beams instead of the three-dimensional beams in static and dynamic analyses. Therefore, the cross-sectional properties such as tension center, shear center and section stiffness of the blades are essential for the analysis. However, it is a difficult task to calculate the cross-sectional properties of the blades.

This paper deals with the development and validation of a general purpose cross-section analysis program KSec2D. The finite element method is used to determine the sectional properties of the composite beams and blades with nonhomogeneous cross-section and nonuniform distribution of material properties. The weighted-modulus approach is adopted to find the properties of the laminated composite material. The shear center is calculated using the Trefftz' definition and the torsion constant is obtained using the St. *Venant* torsion theory. The problem of singular stiffness matrix was encountered in the development stage which was eventually resolved by means of penalty method to eliminate the rigid body mode.

A several number of cross-section profiles are illustrated to validate the current approach, which include two-cell composite airfoil section, small-scale BO-105 blade and KARI (Korea Aerospace Research Institute) small-scaled blade. The cross section properties such as stiffness, shear center offset, tension center offset, center of gravity and inertia properties are obtained using KSec2D and compared with the results obtained using commercial software, the experimental data and with the published data available in the literature. Since, the current version of the cross-section analysis program doesn't support a pre-processor and a post-processor, MD Patran is used as a pre-processor with MD Nastran input file format [4] while the TECPLOT360 [5] is used as the post-processor.

2 Theory

The origin of the user defined coordinate system is considered as reference for an arbitrary cross-section. The coordinates of centroid, tension center and shear center offset, therefore, refer to the user coordinate system. Figure 1 shows the reference axes of the blade. It is assumed that X axis is located at an arbitrary position on the cross-section and X, Y, Z axis are mutually perpendicular to each other. Figure 2 indicates the tension center (T.C.) offset $(\bar{y}, \bar{z})$ and shear modulus weighted centroid (S.M.W.C.) with respect to the reference axis, and shear center (S.C.) offset (y_{sc}, z_{sc}) with respect to the shear modulus weighted centroid.

The tension center offset $(\bar{y}, \bar{z})$ for an isotropic material case can be defined as in Eq. (1), where, A is the area of the cross-section, Q_Y and Q_Z are the first moments of area measured from the reference axes, respectively. In the isotropic material case, tension center coincides with the geometric centroid of the blade cross-section.

$$A = \iint_A dA$$

$$Q_Y = \iint_A z dA, \qquad Q_Z = \iint_A y dA \tag{1}$$

$$\bar{y} = \frac{Q_Z}{A}, \qquad \bar{z} = \frac{Q_Y}{A}$$

The axial (EA) and bending stiffnesses (EI_Y, EI_Z) for the isotropic material case are defined in Eq. (2), where, E is the Young's modulus, I_Y and I_Z are the area moments of the cross-section.

$$EA = E\iint_A dA$$

$$EI_Y = E\iint_A \bar{z}^2 dA\,, \qquad I_Y = \iint_A \bar{z}^2 dA \tag{2}$$

$$EI_Z = E\iint_A \bar{y}^2 dA\,, \qquad I_Z = \iint_A \bar{y}^2 dA$$

The torsion stiffness GJ can be expressed as a function of the shear modulus G and the torsion constant J. Torsion constant can be derived using the St. *Venant* torsion theory [6].

$$J = \iint_A \left[\left(\frac{\partial\omega}{\partial z} + y\right)y - \left(\frac{\partial\omega}{\partial y} - z\right)z\right] dA \tag{3}$$

where, ω is the warping function of the cross-section and the torsion constant J can be determined from the warping function.

The constituents of the cross-section having different properties for a nonhomogeneous cross-section case, the modulus-weighted properties can be expressed with respect to those of the reference sections. For a given segment of the cross-section, the properties are defined in Eq. (4).

$$d\bar{A} = \frac{E_i}{E_0} dA, \qquad d\hat{A} = \frac{G_i}{G_0} dA \tag{4}$$

where, E_0 and $G_0$are the Young's modulus and shear modulus of the reference section, E_i and G_i are the Young's modulus and shear modulus of an ith element.

Using Eq. (4), the section properties modified by modulus-weighted properties are obtained as shown in Eqs. (5) and (6).

$$\begin{aligned} \bar{Q}_Y &= \iint_A z d\bar{A}\,, \qquad \bar{Q}_Z = \iint_A y d\bar{A} \\ \bar{y} &= \frac{\bar{Q}_Z}{\bar{A}}, \qquad \bar{z} = \frac{\bar{Q}_Y}{\bar{A}} \\ \hat{Q}_Y &= \iint_A z d\hat{A}\,, \qquad \hat{Q}_Z = \iint_A y d\hat{A} \\ \hat{y} &= \frac{\hat{Q}_Z}{\hat{A}}, \qquad \hat{z} = \frac{\hat{Q}_Z}{\hat{A}} \end{aligned} \tag{5}$$

In Eq. (5), $\bar{Q}_Y, \bar{Q}_Z$ are Young's modulus weighted first moments of area, and $\bar{y}, \bar{z}$ are Young's modulus weighted centroid. $\hat{Q}_Y, \hat{Q}_Z$ are shear modulus weighted first moments of area, and $\hat{y}, \hat{z}$ are shear modulus weighted centroid.

$$\begin{aligned} \bar{I}_Y &= \iint_A \bar{z}^2 d\bar{A}\,, \qquad \bar{I}_Z = \iint_A \bar{y}^2 d\bar{A} \\ \hat{I}_Y &= \iint_A \hat{z}^2 d\hat{A}\,, \qquad \hat{I}_Z = \iint_A \hat{y}^2 d\hat{A} \end{aligned} \tag{6}$$

In Eq. (6), $\bar{I}_Y, \bar{I}_Z$ and $\hat{I}_Y, \hat{I}_Z$ are Young's modulus weighted and shear modulus weighted moments of inertia, respectively.

Modulus weighted second moments of area with respect to the tension center can be obtained using the parallel axis theorem, expressed in Eq. (7).

$$\begin{aligned} \bar{I}_{\bar{Y}} &= \bar{I}_Y - \frac{\bar{Q}_Y^2}{\bar{A}}, \qquad \bar{I}_{\bar{Z}} = \bar{I}_Z - \frac{\bar{Q}_Z^2}{\bar{A}} \\ \hat{I}_{\hat{Y}} &= \hat{I}_Y - \frac{\hat{Q}_Y^2}{\hat{A}}, \qquad \hat{I}_{\hat{Z}} = \hat{I}_Z - \frac{\hat{Q}_Z^2}{\hat{A}} \end{aligned} \tag{7}$$

In Eq. (7), $\bar{I}_{\bar{Y}}, \bar{I}_{\bar{Z}}$ are Young's modulus weighted area moments of inertia, and $\hat{I}_{\hat{Y}}, \hat{I}_{\hat{Z}}$ are shear modulus weighted area moments of inertia, measured from Young's modulus and shear modulus weighted centroid.

The section stiffness constants of the blade nonhomogeneous materials can be obtained using Eqs. (5) - (6), shown in Eq. (8).

$$\begin{aligned} EA &= E_0 \iint_A d\bar{A} = E_0\bar{A} \\ EI_Y &= E_0\bar{I}_{\bar{Y}} = E_0 \iint_A \bar{z}^2 d\,\bar{A} \\ EI_Z &= E_0\bar{I}_{\bar{Z}} = E_0 \iint_A \bar{y}^2 d\bar{A} \\ GJ &= G_0\hat{J} = G_0\left[\hat{I}_{\hat{Y}} + \hat{I}_{\hat{Z}} - \iint_A \left(\hat{z}\frac{\partial\omega}{\partial y} - \hat{y}\frac{\partial\omega}{\partial z}\right) d\hat{A}\right] \end{aligned} \tag{8}$$

The shear center is defined as a point on the beam cross-section where the applied shear force induces no twist deformation. The elastic strain energy due to pure torsion for a cantilever beam subjected to a twisting moment at its free end is expressed in Eq. (9).

$$U_{torsion} = \frac{L}{2G}\iint_A \left(t_{xy}^2 + t_{xz}^2\right) dA \tag{9}$$

where, t_{xy} and t_{xz} are torsional shear stresses.
The strain energy due to transverse loads V_y and V_z is expressed in Eq. (10).

$$U_{bending} = \frac{1}{2E}\int_L \iint_A \sigma_x^2 dAdx + \frac{L}{2G}\iint_A \left(\tau_{xy}^2 + \tau_{xz}^2\right)dA \quad (10)$$

where, τ_{xy} and τ_{xz} are flexural shear stresses.
The total strain energy due to combined torque and transverse loads is shown in Eq. (11).

$$U = \frac{1}{2E}\int_L \iint_A \sigma_x^2 dAdx + \frac{L}{2G}\iint_A \left\{\left(t_{xy}^2 + t_{xz}^2\right)^2 + \left(\tau_{xy}^2 + \tau_{xz}^2\right)^2\right\}dA \quad (11)$$

The bending and torsion of the beam cross-section can be decoupled by applying load at the shear center location. This decoupled beam has been defined by Trefftz as a torsion-free flexure [6], expressed by a condition in Eq. (12).

$$\iint_A \left(t_{xy}\tau_{xy} + t_{xz}\tau_{xz}\right)dA = 0 \quad (12)$$

The shear stresses due to pure torque as mentioned in [6] are expressed in Eq. (13).

$$t_{xy} = \mathrm{G}\theta\left(\frac{\partial\omega}{\partial y} - z\right), \qquad t_{xz} = \mathrm{G}\theta\left(\frac{\partial\omega}{\partial z} + y\right) \quad (13)$$

Using Eqs. (11) and (12), the Trefftz condition can be written as

$$\iint_A \left(\mathrm{G}\theta\left(\frac{\partial\omega}{\partial y} - z\right)\tau_{xy} + \mathrm{G}\theta\left(\frac{\partial\omega}{\partial z} + y\right)\tau_{xz}\right)dA = 0 \quad (14)$$

Assuming that transverse loads, V_y and V_z are applied at the shear center, Eq. (14) can be expressed as

$$\begin{aligned} y_{sc}V_z &= \iint_A \left(\tau_{xz}y - \tau_{xy}z\right)dA \\ &= -\iint_A \omega\frac{\partial\sigma_x}{\partial x}dA \\ y_{sc}V_z &= \iint_A \omega\frac{V_z}{I_yI_z - I_{yz}^2}\left(I_{yz}y - I_z z\right)dA \\ -z_{sc}V_y &= \iint_A \omega\frac{V_z}{I_yI_z - I_{yz}^2}\left(I_{yz}z - I_y y\right)dA \end{aligned} \quad (15)$$

The above derivation can be extended to nonhomogeneous material case using the modulus-weighted approach. The location of shear center can be derived as

$$\begin{aligned} y_{sc} &= \frac{\hat{I}_{\hat{Z}}\hat{I}_{\hat{Z}\omega} - \hat{I}_{\hat{Y}\hat{Z}}\hat{I}_{\hat{Y}\omega}}{\hat{I}_{\hat{Y}}\hat{I}_{\hat{Z}} - \hat{I}_{\hat{Y}\hat{Z}}^2} \\ z_{sc} &= \frac{\hat{I}_{\hat{Y}\hat{Z}}\hat{I}_{\hat{Z}\omega} - \hat{I}_{\hat{Y}}\hat{I}_{\hat{Y}\omega}}{\hat{I}_{\hat{Y}}\hat{I}_{\hat{Z}} - \hat{I}_{\hat{Y}\hat{Z}}^2} \end{aligned} \quad (16)$$

where, $\hat{I}_{\hat{Y}\omega}$, $\hat{I}_{\hat{Z}\omega}$, $\hat{I}_{\hat{Y}\hat{Z}}$ are the sectorial products of area defined as

$$\hat{I}_{\hat{Y}\omega} = \iint_A \hat{y}\omega d\hat{A}, \qquad \hat{I}_{\hat{Z}\omega} = \iint_A \hat{z}\omega d\hat{A}$$
$$\hat{I}_{\hat{Y}\hat{Z}} = \iint_A \hat{y}\hat{z}d\hat{A} \quad (17)$$

In this work, finite element approach has been used for the cross-sectional analysis of the blades. Three node triangular elements are used to model the complex geometries such as helicopter blades and wind turbine blades, shown in Fig. 3. The cross-section coordinates are transformed into y and z coordinates using shape function N.

$$\mathbf{y} = N(\eta,\zeta)y, \qquad \mathbf{z} = N(\eta,\zeta)z \quad (18)$$

where,

$$N = \lfloor\psi_1 \quad \psi_2 \quad \psi_3\rfloor$$
$$\psi_1 = 1 - \zeta - \eta, \psi_2 = \zeta, \psi_3 = \eta \quad (19)$$

Numerical integration technique is used to obtain the integral of function *f(y,z)* for a cross-section.

$$\iint_A f(y,z)dA = \sum_{i=1}^{n}\int_0^1\int_0^{1-\zeta} f(\eta,\zeta)|J_i|\,d\eta d\zeta \quad (20)$$

where, $|J_i|$ represents the determinant of Jacobian matrix J.
The governing equations of torsional warping ae obtained using the St. *Venant* principle [6], Eq. (21).

$$\iint_A \left[\left(\frac{\partial}{\partial y}\delta\omega\frac{\partial\omega}{\partial y} + \frac{\partial}{\partial z}\delta\omega\frac{\partial\omega}{\partial z}\right) - \left(\frac{\partial}{\partial y}\delta\omega z - \frac{\partial}{\partial z}\delta\omega y\right)\right]dA = 0 \quad (21)$$

where, ω is the warping function, defined for an element as

$$\omega = N\omega_e, \qquad \delta\omega = N\delta\omega_e \tag{22}$$

Eventually, warping equation can be derived using Eqs. (21) and (22).

$$K_e\omega_e - F_e = 0 \tag{23}$$

where, K_e is the element stiffness matrix and F_e is the element load vector defined as

$$\begin{aligned} K_e &= \iint \left(\frac{\partial N^T}{\partial \eta}\frac{\partial N}{\partial \eta} + \frac{\partial N^T}{\partial \zeta}\frac{\partial N}{\partial \zeta} \right) |J| d\eta d\zeta \\ F_e &= \iint \left(\zeta \frac{\partial N^T}{\partial \eta} - \eta \frac{\partial N^T}{\partial \zeta} \right) |J| d\eta d\zeta \end{aligned} \tag{24}$$

3 Results and Discussion

The benchmark tests have been carried out to validate the prediction accuracy of cross-sectional analysis program KSec2D. The cross-section properties which include area centroid, area moment of inertia, torsion constant, shear center offsets and stiffnesses are determined and compared with the results obtained using commercial software and the available experimental data.

3.1 Two-cell airfoil section

Numerical analysis is performed for elastically-coupled composite blades with two-cell airfoil section [7]. The cross-section consists of D-spar having $[0/15]_2$ layup and skin with [15/-15] layup of an orthotropic material. The finite element model for two-celled blade is shown in Fig. 4. The geometric and material properties are presented in Table 1.

In KSec2D, 2,185 3-node triangular elements are used to discretize the cross-section. Inertial properties, stiffness constants and centroidal offsets are compared with the other experimental results, shown in Table 2 [7]. Apparently, a good correlation can be seen compared with the experimental results.

3.2 Small-scale BO-105 blade

The finite element model of small-scale BO-105 blade is shown in Fig. 5. The blade consists of balance weight, actuator, skin, glass solid spar and foam. The chord length is 0.12 m and the total actuator area is 0.16 m^2. The geometry along with tension and shear center offsets is shown in Fig. 5.

The finite element mesh and input file for KSec2D is generated in MD Patran. The material properties of the blade are described in Table 3. The cross-sectional properties such as center of gravity, tension center, shear center offset and section stiffnesses are compared with the experimental results and the numerical results obtained using ANSYS [8], Table 4.

Ksec2D results are obtained using 2,243 3-node triangular elements. The results are in good agreement with those obtained using ANSYS.

3.3 KARI small-scaled blade

The cross-sectional analysis of KARI small-scaled blade is performed using KSec2D. Figure 6 shows the finite element mesh of the blade. KSec2D model is meshed with 2,061 3-node triangular elements. The results are compared with those calculated using CORDAS software (KARI) developed by Russia-Korea Aerospace Research center for composite rotor blade cross-section analysis, shown in Table 5. CORDAS is developed for Windows 98 platform. The finite element mesh and KSec2D input file are generated using MD Patran [9]. An error of 25% is observed for torsion stiffness.

The results are also compared with the experimental data for flap-wise stiffness which varies along the blade span, shown in Fig. 7. A reasonably good correlation can be seen compared with the design values and the experimental results.

4 Conclusions

A finite element-based two-dimensional cross-sectional analysis program KSec2D has been developed. MD Patran is used as a pre-processor and TECPLOT360 is used as a post-processor. The modulus-weighted approach has been used to predict the cross-sectional properties of inhomogeneous composite blades. The classical laminated plate theory (CLPT) is applied to obtain the effective moduli of the walls of composite blades. The torsion constant of the blade cross-section is determined using St. *Venant* torsion theory. The Trefftz' definition is used to find the location of shear center for an arbitrary cross-section.

A series of validation tests have been conducted to substantiate the accuracy of the analysis for various blade cross-sections. A fair to good correlation is achieved for various blade cross-sections as compared to the experimental data and the commercial finite element analysis results. It can be concluded that the KSec2D program shows a good

potential as a cross-section analysis tool for the analysis of arbitrary blade cross-sections in the preliminary design of composite rotor blades.

Acknowledgments

The authors acknowledge the support provided by KARI under the KHP Dual-Use Component Development Program funded by the MKE.

References

[1] http://www.mechatools.com/
[2] http://wind.nrel.gov/
[3] http://www.sandia.gov/
[4] MD Nastran R2.1, MSC Software Corporation, Santa Ana, CA, 2008.
[5] http://www.tecplot.com/products/360/
[6] W. D. Pilkey "*Analysis and design of elastic beams*". John Wiley & Sons, Inc., 2002.
[7] R. Chandra and I. Chopra "Structural behavior of two-cell composite rotor blades with elastic couplings". *AIAA Journal*, Vol. 30, No. 12, pp 2914-2921, 1992.
[8] 1st DLR/KU MOU Meeting, Dec. 9-11, 2008.
[9] MD Patran R2.1, MSC Software Corporation, Santa Ana, CA, 2008.

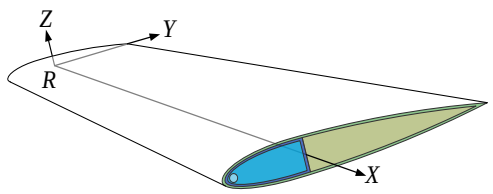

Fig.1. Reference axes of the blade.

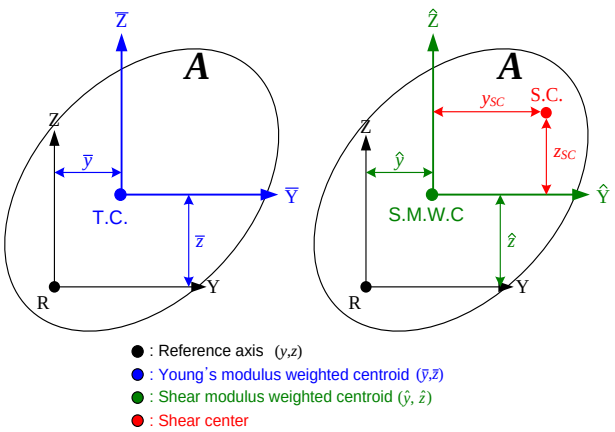

Fig.2. Coordinate systems of a blade cross-section.

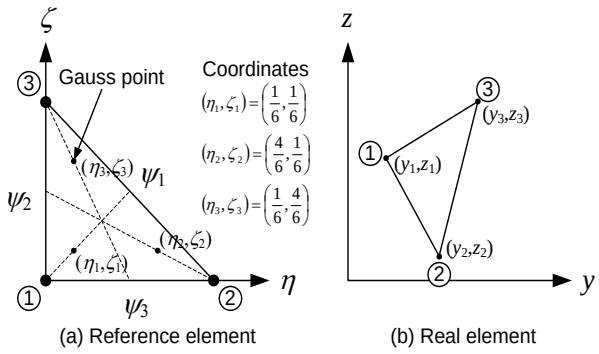

Fig.3. Gauss integration order and location of integration points for 3-node triangular element.

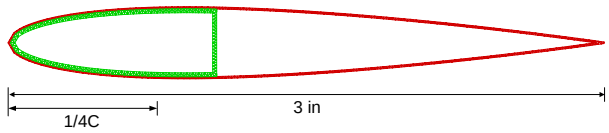

Fig.4. Finite element mesh of a two-cell airfoil section.

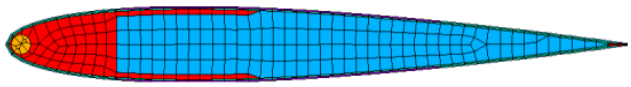

(a) ANSYS model [8].

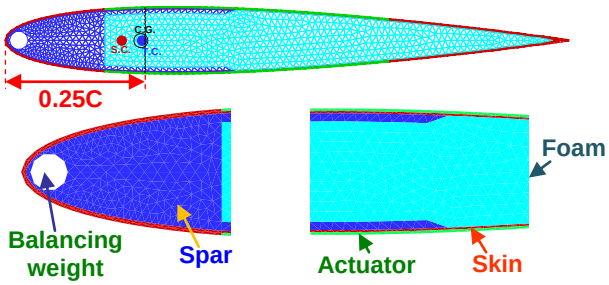

(b) KSec2D model.

Fig.5. FE meshes and profiles of small-scale BO-105 blade in (a) ANSYS, and (b) KSec2D.

Fig.6. FE meshes of KARI small-scaled blade in KSec2D.

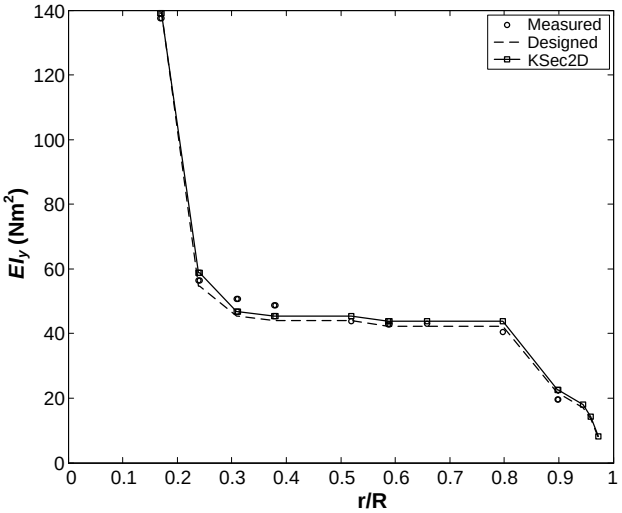

Fig.7. Comparison of KSec2D results with the experimental data for flap-wise stiffness along the blade span.

Table 1. Geometric and material properties of two-cell airfoil section composite blade.

Properties	Values
E_1	131 GPa
E_2	9.3 GPa
G_{12}	5.86 GPa
ν_{12}	0.40
Ply thickness	0.127 mm
Airfoil	NACA 0012
Length	641.4 mm
Chord	76.2 mm
Airfoil thickness	9.144 mm

Table 2. Comparison of cross-sectional properties of a two-cell airfoil section.

$\theta = 15°$			KSec2D	Chandra and Chopra [7]	% error
Section Stiffness	EA (N)		7.3840E+06	-	-
	EI_Y (N-m^2)		7.9408E+01	7.7141E+01	2.94
	EI_Z (N-m^2)		3.2085E+03	-	-
	GJ (N-m^2)		2.5662E+01	2.5427E+01	0.93
Offset	Tension center (m)	y-dir	2.7661E-02	-	-
		z-dir	0.0000E+00	-	-
	Shear center (m)	y-dir	1.6825E-02	-	-
		z-dir	0.0000E+00	-	-

Table 3. Material properties of small-scale BO-105 blade.

Properties	CFRP	MFC actuator	Foam	Balance weight
E_1 (N-m^2)	45.166x10^9	30.0 x10^9	0.035x10^9	-
E_2 (N-m^2)	11.981x10^9	15.5x10^9	0.035x10^9	-
G_{12} (N-m^2)	4.583x10^9	10.7x10^9	0.014x10^9	-
ν_{12}	0.238	0.4	0.25	-
ρ (kg/m^3)	2,008	4,700	52	19,250
		Ply orientation		
Skin		+30°		
MFC		-40°		

Table 4. Cross-sectional properties of small-scale BO-105 blade.

Properties		Experiment [8]	ANSYS [8]	KSec2D
Center of gravity offset (m)	y-dir	-	2.93E-02	2.91E-02
	z-dir	-	3.62E-08	2.19E-07
Tension center offset (m)	y-dir	-	-	2.94E+02
	z-dir	-	-	2.39E-07
Shear center offset (m)	y-dir	-	1.96E-02	2.50E-02
	z-dir	-	7.23E-03	5.64E-07
Section stiffness	EA (N)	-	1.43E+07	1.45E+07
	EI_Y (N-m^2)	1.97E+02	2.37E+02	2.68E+02
	EI_Z (N-m^2)	-	8.42E+03	1.08E+04
	GJ (N-m^2)	1.94E+02	1.71E+02	1.64E+02

Table 5. Cross-sectional properties of KARI small-scaled blade.

Properties		CORDAS (KARI)	KSec2D	% error
Tension center offset (m)	y-dir	0.2023	0.2179	0.0199C
	z-dir	0.0013	0.0022	0.0011C
Shear center offset (m)	y-dir	0.1927	0.2250	0.0411C
	z-dir	0.0024	0.0021	0.0004C
Section stiffness	EA (N)	5.07E+06	5.29E+06	4.34
	EI_Y (N-m^2)	5.45E+01	5.70E+01	4.59
	EI_Z (N-m^2)	2.22E+03	2.33E+03	4.95
	GJ (N-m^2)	6.74E+01	8.42E+01	24.93